2024 IEEE/RSJ International Conference on Intelligent Robots and Systems (IROS)
October 14-18, 2024. Abu Dhabi, UAE

A Biomimetic Robot Crawling Upstream using Adhesive Suckers Inspired by Net-winged Midge Larvae

Haoyuan Xu, Shuyong Zhao, Jiale Zhi, Chongze Bi, and Li Wen

***Abstract*— Net-winged midge larvae (genus Liponeura) can achieve robust attachment and crawl on the slippery surface in the fast stream with their powerful abdominal suckers. The rigid spine-like structures distributed in the sucker cavity called microtrichia, have been proven to be crucial in the adhesion process. In this work, we carry out a design of the biomimetic sucker with the spine-like structures and then implement various tests using biomimetic suckers to verify the adhesion capacity enhancement brought by spine-like structures. Finally, we assemble the suckers in a quadruped crawling robot capable of locomotion in both aerial and aquatic environments with a speed of 56.4 mm/s (0.225 BL/s) and can crawl upstream against a turbulent flow with a speed of 38.2 mm/s (0.152 BL/s). This study will inspire biomimetic design in future robotics, and pave the way for future robots to realize long-term observation and monitoring in complex environments.**

***Index Terms*— Attachment and detachment, Soft adhesive, Crawling robot**

I. Introduction

In the past few years scientists have found that the net-winged midge larvae can firmly attach to the rocks at the bottom of fast streams in the mountains. In this challenging environment, the water velocity can reach 3 m/s [1], such a harsh environment allows the net-winged midge larvae to avoid the predation of natural enemies. Individual net-winged midge larvae adhere so strongly that they require a force more than 600 times their body weight to separate vertically from a rock, which is the strongest adhesion that an insect can realize known by people so far.

Previous studies reveal that three components play essential roles in adhesion [2]: the V-shaped gap on the sucker rim (V-notch), the cylinder-like structure (Piston) located at the central cavity, and the circularly distributed microtrichia on the bottom surface of the sucker. In 2002, A. Frutiger present an accurate description of the sucker of net-winged midge larvae [3], clarifying that the function of a piston-like structure is to create negative pressure in the adhesion process. Also, V. Kang summarized that the V-notch functions as a water channel to release pressure [1]. In the follow-up work, he study the morphology and ultrastructure of midges larvae's sucker using freeze-fracture scanning electron microscopy (SEM), and X-ray computed micro-tomography (micro-CT) [4]. The results indicate that there are rim microtrichia repeated around the perimeter of the disc, forming a continuous region of close contact around the attachment organ.

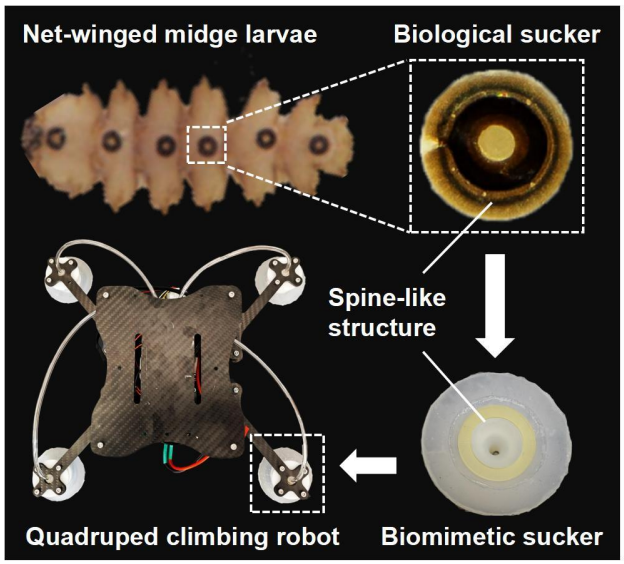

Fig. 1. Quadruped crawling robot equipped with four biomimetic suckers inspired by net-winged midge larvae.

Significant progress has been made in understanding the morphology of the suckers of net-winged midges. However, biomimetic studies specifically focusing on these suckers have yet to be realized. Our previous research has investigated the piston and V-notch structures of the midge sucker through biomimetic approaches, and clarified that the V-notch structure brings mechanical anisotropy to the sucker [5]. Nevertheless, essential questions regarding the microtrichia on the suckers remain unanswered. How does the presence of microtrichia contribute to increased adhesion? Furthermore, how can such biomimetic suckers equipped with microtrichia be effectively translated into practical applications within the field of robotics? Reliable and reversible adhesion has attracted growing attention in the field of bio-robotics in recent year [6]–[9], thus understanding the mechanism of net-winged midge larvae sucker may

This work was supported by: the National Key R&D Program of China (Grant Nos. 2022YFB4701800), and National Science Foundation support projects, China (Grant Nos. T2121003, 92048302).*(Corresponding author: Li Wen)*

Haoyuan Xu is with the School of Mechanical Engineering and Automation, Beihang University, Beijing 100083, P.R. China, and also with the ShenYuan Honors College, Beihang University, Beijing 100083, China (e-mail: xhy121yhx@buaa.edu.cn).

Shuyong Zhao, Chongze Bi, and Li Wen are with the School of Mechanical Engineering and Automation, Beihang University, Beijing 100083, China (email: zh_3974@outlook.com; 21374110@buaa.edu.cn; liwen@buaa.edu.cn).

Jiale Zhi is with the School of CENTRALE PEKINSchool of General Engineering, Beihang University, Beijing 100083, China (e-mail: 1397430395@buaa.edu.cn).

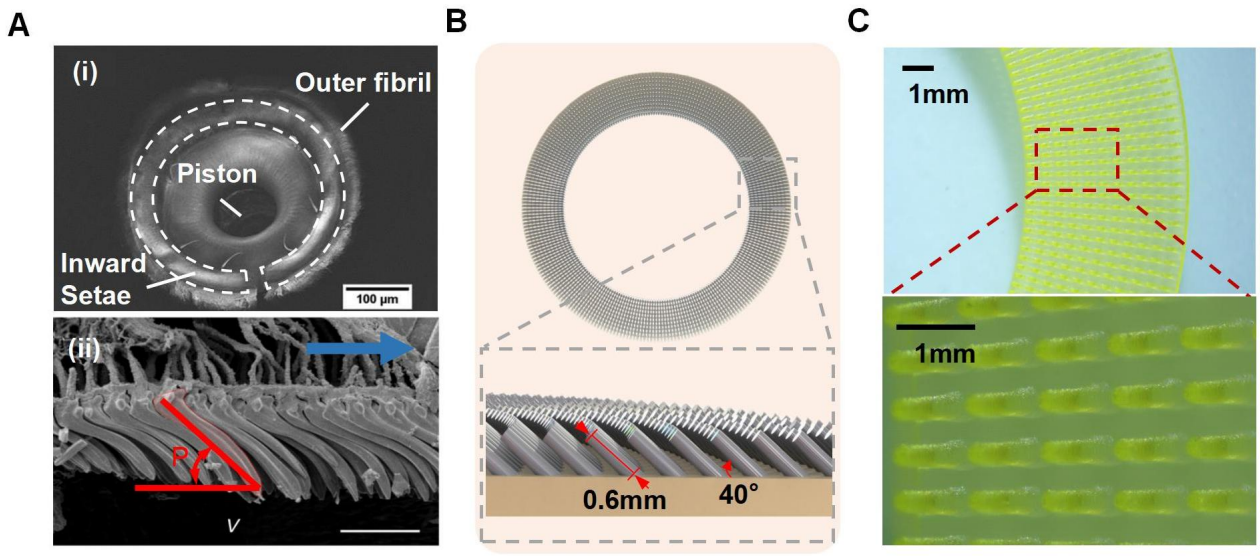

Fig. 2. Biological and biomimetic microstructure of net-winged midge larvae sucker. (A) (i) SEM image of a sucker of net-winged midge larvae. The white dotted area is the inward setae area. (ii) Freeze-fracture SEM of inward setae on a sucker showing the pitch angle (shaded in red). Arrow points toward the center of the sucker. V: ventral. Scale bar: 5 μm. SEM images: Reproduced with permission of Ref. 11, Copyright 2021, eLife. (B) 3D model of the biomimetic micro-structure ring. (C) Images of the microstructure ring taken by optical microscope.

serve as a new source of inspiration for the development of future robots.

In this work, we present a novel biomimetic sucker featuring functional spine-like structures to replicate and investigate the biological adhesion mechanism of the midges (Fig.1). Firstly, we detail the design and fabrication process of the biomimetic sucker. Then, we analyze the adhesion enhancement mechanism of the sucker and implement the Frustrated Total Internal Reflection (FTIR) experiment to validate our findings. Quantitatively, we give a comparative experiment of the pull-off force and friction force of the biomimetic sucker with the oridinary sucker. Furthermore, we evaluate the performance of the suction cups under real-world conditions, subjecting them to normal loads (lifting heavy objects) and tangential loads (resisting water flow impacts). Finally, we integrate the biomimetic suckers into a quadruped crawling robot (Fig.1), showcasing its agile and versatile movement capabilities across various media and against turbulent flow.

II. Modeling and Design

A. Design of the Micro-structure

On the ventral surface of the net-winged midge larvae's sucker, there is a circular area containing rim microtrichia, also known as inward setae (Fig. 2(A)). These rim microtrichia repeated around the perimeter of the sucker, forming a continuous region of close contact when the sucker is in close attachment. Also, the microstructure in the sucker of midges is distributed in a ring and points to the center of the sucker with a pitch angle of 40°, capable of generating friction force in any direction [1]. According to the research of V. Kang et al., [4], Young's modulus of these microstructures is at least 0.3–0.4 GPa, similar to the stiffness of wood and bone.

To verify the effect of microstructure on net-winged midge larva's suckers, a microstructure model that is morphologically similar to the midge's sucker is designed. From previous research [1], the aspect ratio (length: diameter) of the microtrichia is 5:1, and the length of a single microtrichia to the sucker diameter is about 1:100. Following these morphological principles, a biomimetic microstructure ring, with thousands of micro setae (length: 0.6mm, pitch angle: 40°) distributed in a circular pattern is designed, as shown in Fig.2(B). With the technology of microscale additive manufacturing, a resin microstructure ring is produced. Fig.2(C) shows the image of the ring under an optical microscope.

B. Fabrication of the Biomimetic Sucker

The biomimetic sucker consists of three components (Fig.3): the main body, a soft lip ring, and microstructures, with dimensions measuring 60 mm (length) × 60 mm (width) × 27 mm (height). The contact area of the sucker is 24.47 cm^2. The main body is cast using silicone material (Dragon Skin 20, Smooth-ON), the flexible lip ring is cast using silicone material (Ecoflex 10, Smooth-ON), and the microstructures are fabricated using microscale additive manufacturing. Finally, assembly is completed using silicone adhesive.

C. Analysis of the Adhesion-Enhancement Mechanism

When the sucker is in a detached state (Fig. 4(A)), there is no pressure differential between the inside and outside of the sucker chamber, and its shape remains in its original state. However, when the gas inside the sucker is evacuated (Fig. 4(B)), a pressure differential is established between the inside and outside of the sucker, leading the lip to be pressed against the substrate, resulting in compression of the microfibers and interlocking with the substrate. At this time, when

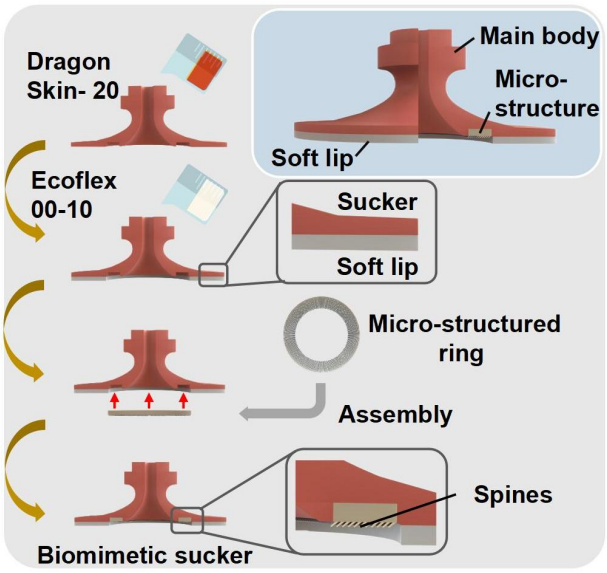

Fig. 3. Multistep manufacturing process of the biomimetic sucker. Step 1: The main body of the sucker is cast from a mold with Dragon Skin 20 silicone. Step 2: A thin soft layer is cast with Ecoflex 00-10 silicone and glued together with the main body. Step 3: The sucker and the micro-structure ring are assembled with adhesive material.

the biomimetic sucker is pulled in the normal direction with a force of F_p (Fig. 4(C)), the contact area between the sucker and the substrate surface is pulled inward towards the center of the cup base. As the pulling force increases, the contact area begins to slide on the substrate surface. Nevertheless, the spines on the micro-structured ring are oriented inwardly, which is believed to increase the shear strength f_1 and prevent slipping. Similarly, when the biomimetic sucker is pulled in the shear direction with a force of F_s (Fig. 4(C)), the fibers can enhance the effective friction coefficient of the contact surface to resist the shear force.

D. Design of the Adhesive Crawling Robot

To demonstrate the performance of the biomimetic sucker, we designed an untethered quadruped crawling robot utilizing the sucker as the adhesive pad. The suckers are actuated by a diaphragm pump capable of generating a negative pressure of 40 kPa and are controlled by four solenoid valves integrated into the robot (Fig.5(A)). The legs module of the robot has a parallelogram four-bar linkage mechanism that was actuated by a servo motor (Fig.5(B)). Fig.5(C) illustrates the schematic diagram of the parallelogram four-bar linkage mechanism. The length of the coupler $l_1 = 38mm$ and the length of the rocker $l_2 = 27mm$. As the servo motor rotates, the trajectory of the end is a circle whose diameter is $d_2 = 54mm$, indicating the farthest distance the robot can make by one step. Under the manipulation of a special-designed circuit board, the legs rotate and the suckers adhere and detach sequentially, driving the whole robot to crawl along the Y-axis (Fig.5(D)) and the X-axis (Fig.5(E)).

When crawling along the Y-axis, initially, the suckers on Leg2 and Leg3 attach and the suckers on Leg1 and Leg4

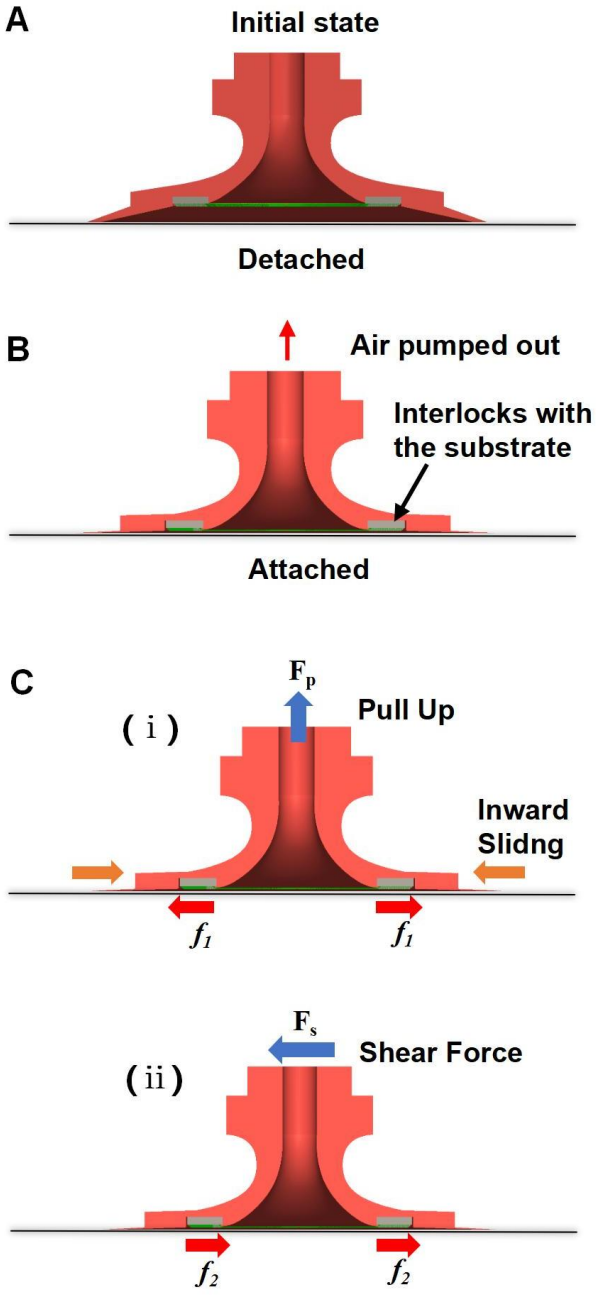

Fig. 4. Illustration of the mechanism of micro-structure in the sucker. (A) At the initial state, the sucker is placed on the plane with its original shape. (B) The negative is produced within the suction chamber, causing the deformation of the sucker. (C) Schematic illustration of the principle of micro-structure increasing the adhesion capacity of sucker. F_p represents the pull-up force caused by the normal load. f_1 represents the friction force derived from the spine structure to resist the inward sliding tendency. (D) Schematic illustration of the principle of micro-structure increasing the friction capacity of the sucker.F_s represents the shear force caused by the tangential load. f_2 represents the friction force derived from spine structure.

detach (Fig.5(D) stage 1), then the four servo motors rotate counter-clockwise until legs on the right side exceed the left ones (Fig.5(D) stage 3). Next, the suckers on Leg1 and Leg4 attach and the suckers on Leg2 and Leg3 detach, the four servo motors rotate clockwise until the left legs exceed the left ones. When crawling along X-axis, the suckers on Leg1 and Leg4 attach and the suckers on Leg2 and Leg3 detach at first (Fig.5(E) stage 1), then the four servo motors rotate counter-clockwise (clockwise would also take effect) until the robot "folds" (Fig.5(E) stage 3). Then the suckers on Leg2 and Leg3 attach and the suckers on Leg1 and Leg4 detach, the servos rotate to the initial "expanded" state, making the robot moves one step.

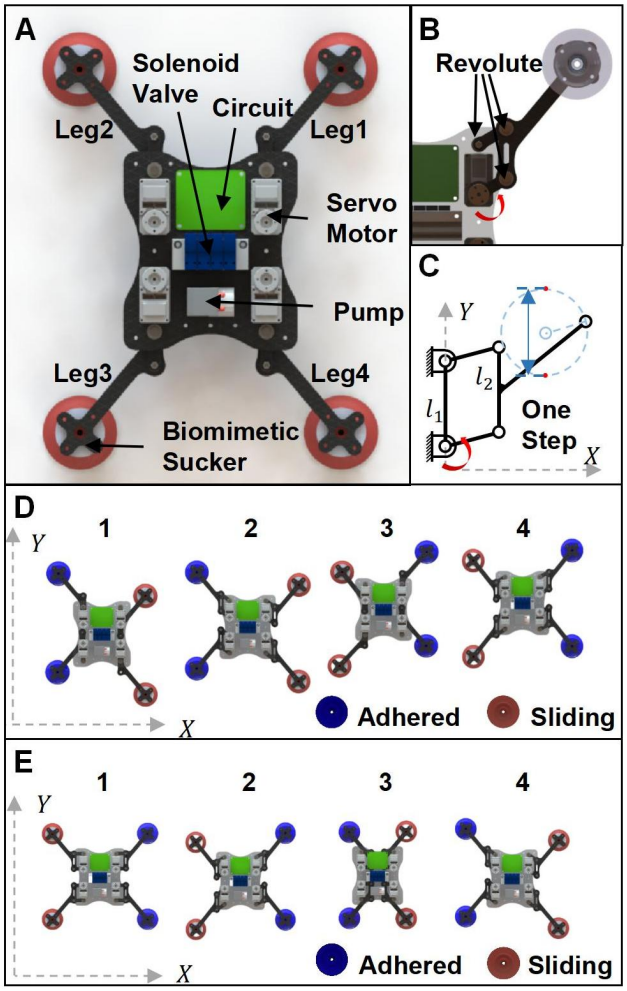

Fig. 5. Overview of the climbing robot. (A) An overall view of the robot from the top. (B) Parallelogram four-link mechanism of robot's leg. The red curled arrow refers to actuation. (C) Schematic diagram of the four-link mechanism. The trajectory of the end is a circle. (D) The y-oriented crawling pace of the robot. (E) The x-oriented crawling pace of the robot

III. Experiment Results

A. FTIR Experiment of the Biomimetic Sucker

To understand how the spine-like structure enhances friction during attachment, we characterized the contact between the biomimetic sucker and the substrate under different

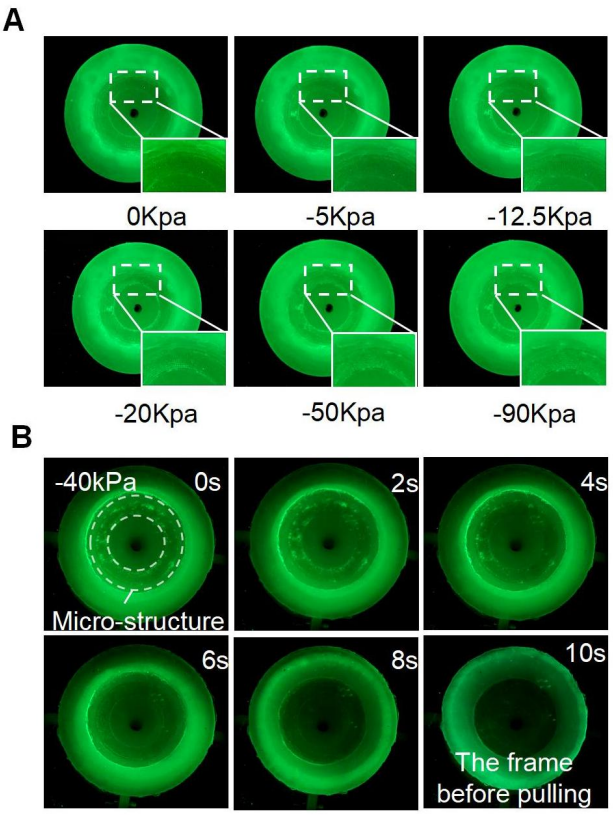

Fig. 6. The FTIR Experiment of the biomimetic sucker (A) The images of the biomimetic sucker under different negative pressures. The same area in the different image is zoomed in to display the contact condition of the microstructure. (B) A series of FTIR images of the sucker's pull-off process. A Grey dotted ring surrounds the micro-structure area.

negative pressure states (Fig.6(A)). Under a 0 kPa condition, there is no contact between the spine structure region of the sucker and the substrate. As the pressure differential between the inside and outside increases, the contact between the spine structure region and the substrate gradually transitions from internal to external compression, forming interlock.

When the pressure differential exceeds 20 kPa, almost the entire spine-like structure region comes into contact with the substrate. From the above, it can be concluded that when the sucker is not activated, the spine structure of the sucker does not contact the surface, remaining in a low-friction state. However, under significant negative pressure (>20 kPa), the spine-like structure structure of the sucker is fully engaged with the substrate, resulting in a high-friction state. By altering the internal pressure of the sucker (via pump, piston), the transition between high and low-friction states of the sucker can be achieved.

Additionally, we characterized the detachment process in the normal direction when the sucker is in the activated state (under -40 kPa) (Fig.6(B)). From 0 to 4 seconds, the spines gradually detach from the substrate; subsequently, from 4 to 10 seconds, the lip of the sucker gradually deforms inward, eventually leading to the rupture of the sucker seal and detachment from the surface. The result demonstrates that the rigidity of the spine-like structure and interlocking

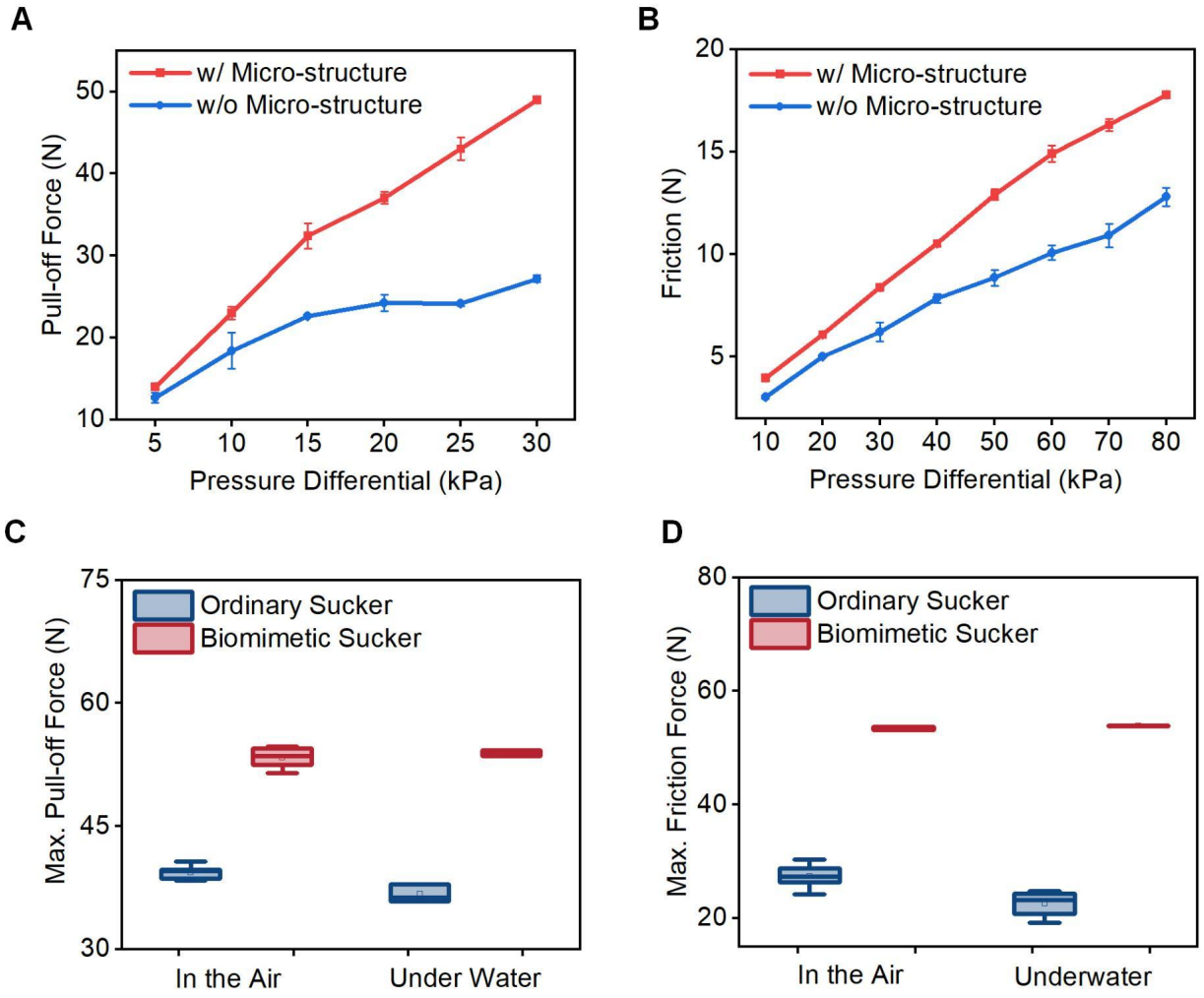

Fig. 7. Mechanical comparison testing of biomimetic suckers (A) The relationship between negative pressure and pull-off force for suckers with and without micro-structure. w/ Micro-structure: with micro-structure. w/o Micro-structure: without Micro-structure. (B) The relationship between negative pressure and friction force for suckers with and without micro-structure. (C) Comparison of maximum pull-off force between the biomimetic sucker and ordinary sucker in the air and underwater. (D) Comparison of maximum friction force between the biomimetic sucker and ordinary sucker in the air and underwater. The error bars represent one standard deviation (n=5).

mechanisms restrict the tendency of the sucker to slide inward, thereby increasing the normal detachment force of the sucker.

B. Adhesive Performance of the Biomimetic Sucker

To further validate the enhancement of suction performance by spine-like structures, we conducted tests comparing biomimetic suckers with spine-like structures (w/Micro-structure) to ordinary suckers without spine-like structures (w/o Micro-structure). We measured their normal detachment forces (Fig. 7(A)) and frictional forces (Fig. 7(B)) under various negative pressures. The results indicate that the spine-like structures significantly improve both the normal detachment force and frictional force of the sucker. As the pressure differential increases, there is a corresponding increase in the differential between the pull-off force and the frictional force. This observation aligns with the mechanism of adhesion enhancement in Fig.4(C). Additionally, we evaluated the maximum normal detachment force (Fig. 7(C)) and maximum frictional force (Fig. 7(D)) of different suckers, all driven by the same diaphragm pump capable of generating a negative pressure of 40 kPa, in both air and underwater conditions. the findings indicate that the biomimetic sucker consistently outperforms the ordinary sucker (without microstructure) in terms of overall adhesion performance.

C. Comprehensive Testing of Biomimetic Sucker

To verify the benefits conferred by spine-like structures on biomimetic suckers, comparative tests were conducted between biomimetic suckers and ordinary suckers (Supplement video). Under constant negative pressure of -30 kPa, the biomimetic suckers effortlessly lift weights of up to 4 kg with minimal deformation observed at the rim (Fig. 8(A)). Conversely, the ordinary sucker fails to lift weights of 4 kg under the same pressure (Fig. 8(B)). Significant deformation

is observed at the rim of the ordinary sucker, indicating that the weight exceeds the structural limit of the sucker. To evaluate the performance of the biomimetic sucker in turbulent environments, a water flow test was conducted. Fig.8(C) demonstrates that the sucker can withstand flow impact at velocities of up to 1.7 m/s without displacement (Supplement video).

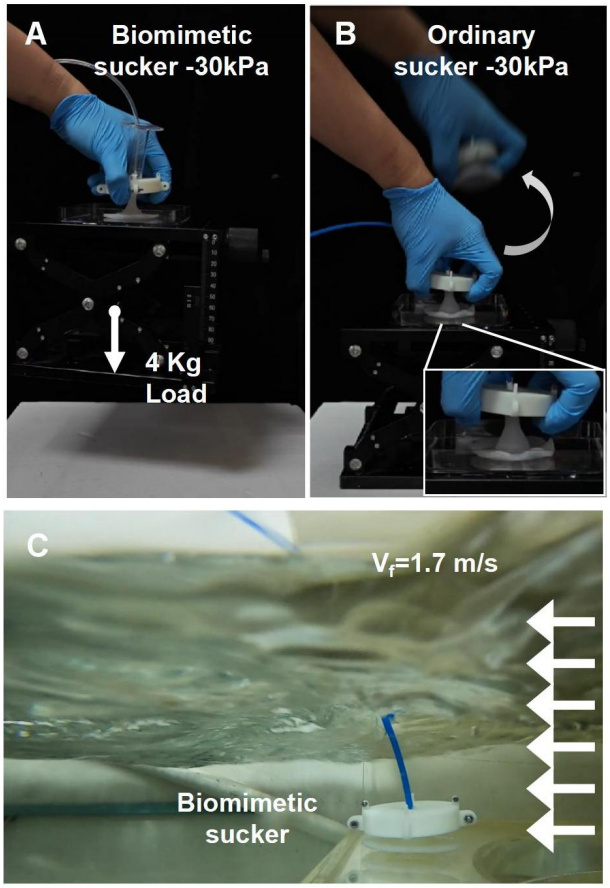

Fig. 8. The comprehensive test of biomimetic sucker (A) Biomimetic sucker lifts weights of 4 Kg. Constant negative pressure: -30 kPa. (B) ordinary sucker(same shape as biomimetic sucker but without microstructure ring) fails in lifting weights of 4 Kg. Constant negative pressure: -30kPa. The curved arrow indicates the movement of the human hand. (C) Biomimetic sucker water flow test. Flow velocity: 1.7 m/s.

D. Performance Evaluation of the Crawling Robot

The crawling robot's performance was evaluated by testing its locomotion capabilities on dry surfaces (Supplementary Video). It achieved a crawling speed of up to 56.4 mm/s (0.225 BL/s) and demonstrated stable forward and backward movement. To validate the locomotion abilities of the biomimetic climbing robot in complex environments, we conducted experiments where the robot traversed a half-immersed slope with the suction cups initially fully immersed in water (Fig. 9A). The results indicate that the robot successfully crawled along the slope, traversed the water-air boundary, and ultimately emerged completely from the water (Supplementary Video). Also, We conducted tests on the robot's resistance to water flow impact in a recirculating water tank. The results demonstrate that the robot can crawl upstream against the flow along a smooth acrylic incline (slope: 8 degrees) with a speed of 38.2 mm/s (0.152 BL/s).

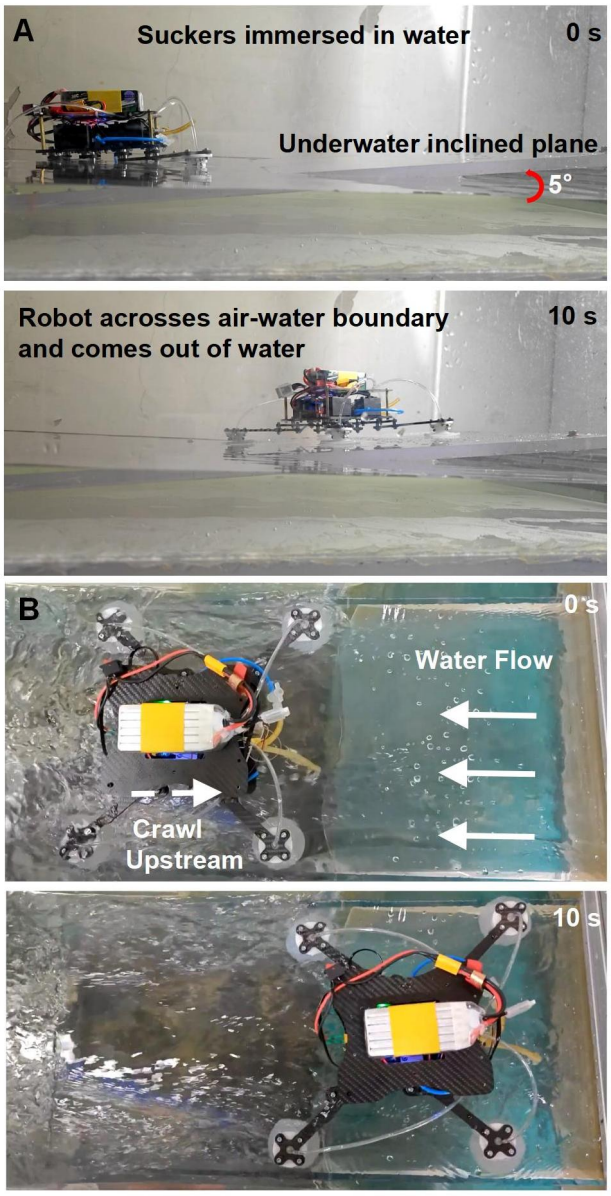

Fig. 9. Comprehensive performance test of the robot (A) The robot crawls across the air-water boundary on a half-immersed inclined plane. Inclined angle: 5°. (B) The robot crawls upstream against a turbulent flow on the acrylic slope. Inclined angle: 8°.

IV. Conclusions

In this work, we introduce a biomimetic sucker design with micro-structure to explore the adhesion enhancement mechanism of the spine-like structures (microtrichia) based on the morphological features of the net-winged midge larvae' sucker. Then, we integrate the biomimetic suckers into a quadruped crawling robot to achieve the practical robotics applications of the biomimetic sucker.

TABLE I

COMPARISON OF OUR ROBOT WITH SIMILAR ADHESIVE CRAWLING ROBOTS IN LITERATURE

Crawling Robot	Tethered	Amphibious	Actuation Method	Maximum Speed (BL/s)	Self-weight (g)	Inclined Plane
Our Robot	**No**	**Yes**	**Motor**	**0.225**	**1320**	**Yes**
Kim et al. [10]	No	No	Motor	0.12	370	Yes
Ta et al. [11]	Yes	No	Motor	0.1733	238	No
Dong et al. [12]	No	No	Passive	0.082	684	Yes
Tolley et al. [13]	No	Yes	Pneumatic	0.0377	3800	No
Duggan et al. [14]	No	No	Pneumatic	0.0033	70.4	No
Zou et al. [15]	Yes	No	Pneumatic	0.0333	230	No
Qin et al. [16]	Yes	No	Pneumatic	0.12	43.5	Yes
Tang et al. [17]	Yes	Yes	Pneumatic	0.0267	10	Yes

Our experimental results lead to the following contributions: (1) The spine-like structures enhance the adhesion capacity of the biomimetic sucker by effectively increasing friction and preventing slipping in both normal and shear directions. (2) The spine-like structures can greatly improve the sucker's friction force (up to 259%) and detachment force (up to 146%). (3) The biomimetic quadrupedal crawling robot is capable of stable locomotion at a speed of 56.4 mm/s (0.225 BL/s) in both dry and wet slippery environments. (4) The robot can crawl upstream against the turbulent flow with a speed of 38.2 mm/s (0.152 BL/s).

Besides, we test the comprehensive adhesive stability of the biomimetic sucker. Compared to the ordinary suckers (without spine-like structures), the biomimetic suckers can lift weights of at least 4 kg. In turbulent flow test ($V_f = 1.7m/s$), the sucker can firmly attach to the surface of the tank without being washed away, proving its reliable underwater adhesion performance. Also, we summarize and compare our quadrupedal crawling robot with other crawling robots equipped with adhesive pads in literature [10]–[17], as in Table I. The results indicate that our robot exhibits high integration, fast locomotion speed, and good environmental adaptability.

In summary, our study represents an advancement in the field of biomimetic robots by translating the unique adhesion enhancement mechanism of midge-like suckers into functional, robust, and agile crawling robots capable of operating in challenging environments. Future work could focus on design optimization for more specific robotic tasks, integration of sensory feedback, and controllable locomotion in complex environments.

ACKNOWLEDGMENT

We thank SiQi Wang, Bocheng Tian, and Fuqiang Yang for their assistance in designing and fabricating the sucker prototype and force experiments.

REFERENCES

[1] V. Kang, R. Johnston, T. van de Kamp, T. Faragó, and W. Federle, "Sophisticated suction organs from insects living in raging torrents: Morphology and ultrastructure of the attachment devices of net-winged midge larvae (Diptera: Blephariceridae)," bioRxiv, p. 666537, 2019.

[2] P. Zwick, "Insecta: Diptera, Blephariceridae," Academy of Sciences Malaysia, vol. 10, pp. 736–749, 2004.

[3] A. Frutiger, "The function of the suckers of larval net-winged midges (Diptera: Blephariceridae)," Freshwater Biology, vol. 47, no. 2, pp. 293–302, 2002.

[4] V. Kang, R. T. White, S. Chen, and W. Federle, "Extreme suction attachment performance from specialised insects living in mountain streams (Diptera: Blephariceridae)," Elife, vol. 10, p. e63250, 2021.

[5] H. Xu, F. Yang, Y. Zhang, X. Jiang, and L. Wen, "A biomimetic suction cup with a V-notch structure inspired by the net-winged midge larvae," IEEE Robotics and Automation Letters, vol. 7, no. 2, pp. 3547–3554, 2022.

[6] G. Picardi, M. Chellapurath, S. Iacoponi, S. Stefanni, C. Laschi, and M. Calisti, "Bioinspired underwater legged robot for seabed exploration with low environmental disturbance," Science Robotics, vol. 5, no. 42, p. eaaz1012, 2020.

[7] L. Li et al., "Aerial-aquatic robots capable of crossing the air-water boundary and hitchhiking on surfaces," Science Robotics, vol. 7, no. 66, p. eabm6695, 2022.

[8] W. Tan et al., "Uncover rock-climbing fish's secret of balancing tight adhesion and fast sliding for bioinspired robots," National Science Review, vol. 10, no. 8, p. nwad183, 2023.

[9] B. Tao, Z. Gong, and H. Ding, "Climbing robots for manufacturing," National Science Review, vol. 10, no. 5, p. nwad042, 2023.

[10] S. Kim, M. Spenko, S. Trujillo, B. Heyneman, D. Santos, and M. R. Cutkosky, "Smooth vertical surface climbing with directional adhesion," IEEE Transactions on robotics, vol. 24, no. 1, pp. 65-74, 2008.

[11] T. D. Ta, T. Umedachi, and Y. Kawahara, "Design of frictional 2D-anisotropy surface for wriggle locomotion of printable soft-bodied robots," in 2018 IEEE International Conference on Robotics and Automation (ICRA), IEEE, 2018, pp. 6779–6785.

[12] X. Dong, C. Tang, S. Jiang, Q. Shao, and H. Zhao, "Increasing the payload and terrain adaptivity of an untethered crawling robot via soft-rigid coupled linear actuators," IEEE Robotics and Automation Letters, vol. 6, no. 2, pp. 2405–2412, 2021.

[13] T. Tolley Michael, F. Shepherd Robert, C. Galloway Kevin, J. Wood Robert, and M. Whitesides George, "A resilient, untethered soft robot," Soft robotics, 2014.

[14] T. Duggan, L. Horowitz, A. Ulug, E. Baker, and K. Petersen, "Inchworm-inspired locomotion in untethered soft robots," in 2019 2nd IEEE International Conference on Soft Robotics (RoboSoft), IEEE, 2019, pp. 200–205.

[15] J. Zou, Y. Lin, C. Ji, and H. Yang, "A reconfigurable omnidirectional soft robot based on caterpillar locomotion," Soft robotics, vol. 5, no. 2, pp. 164–174, 2018.

[16] L. Qin, X. Liang, H. Huang, C. K. Chui, R. C.-H. Yeow, and J. Zhu, "A versatile soft crawling robot with rapid locomotion," Soft robotics, vol. 6, no. 4, pp. 455–467, 2019.

[17] Y. Tang, Q. Zhang, G. Lin, and J. Yin, "Switchable adhesion actuator for amphibious climbing soft robot," Soft robotics, vol. 5, no. 5, pp. 592–600, 2018.